# Mathematical Models for the Accuracy of the Estimated Distribution of Primary Activity Times in Dynamic Spectrum Access Systems

Miguel López-Benítez[†‡], Ogeen H. Toma[†] and Dhaval K. Patel[*]
[†]Department of Electrical Engineering and Electronics, University of Liverpool, United Kingdom
[‡]ARIES Research Centre, Antonio de Nebrija University, Spain
[*]School of Engineering and Applied Science, Ahmedabad University, India
Email: m.lopez-benitez@liverpool.ac.uk, ogeen.toma@liverpool.ac.uk, dhaval.patel@ahduni.edu.in

***Abstract*—Dynamic Spectrum Access (DSA) / Cognitive Radio (CR) systems can greatly benefit from the knowledge of the activity statistics of the primary channel. Such statistics can be estimated by the DSA/CR system based on the on/off decisions provided by the employed spectrum sensing algorithm, which can be processed to estimate the duration of the individual idle/busy periods of the primary channel and subsequently a broad range of activity statistics. Previous work has investigated analytically this estimation approach and provided closed-form expressions for the estimated distribution as well as its associated estimation error. However, existing analytical results are provided in an implicit form that requires some form of numerical evaluation and is not always well-suited for analytical manipulations. In this context, this work extends the existing results by providing mathematical models in an explicit form that can be evaluated directly and are applicable to several estimation strategies. The obtained mathematical expressions are validated with simulation results, showing a remarkable high level of accuracy.**

## I. Introduction

Despite being a broader concept [1], [2], Dynamic Spectrum Access/Cognitive Radio (DSA/CR) [3] is commonly understood as an opportunistic spectrum access paradigm where unlicensed (secondary) users can access frequency bands allocated to licensed (primary) users during those intervals that the channel is inactive (i.e., not being used for transmission by the primary users). Given the opportunistic nature of this spectrum access approach, the performance of DSA/CR systems depends on the spectrum occupancy pattern of primary systems. For this reason, DSA/CR systems can benefit enormously from the knowledge of primary activity statistics. Statistical information such as the durations of the idle/busy periods of the primary channel and their underlying distributions can be exploited by DSA/CR systems to predict future spectrum occupancy trends [4], select the most convenient licensed frequency band and radio channel of operation [5], and for other spectrum and radio resource management decisions that can help minimise interference, optimise the system performance and improve the overal spectrum efficiency [6].

The activity statistics of a primary channel can be estimated by DSA/CR systems based on the outcomes of the spectrum sensing process [7]. The main purpose of spectrum sensing in a DSA/CR system is to determine the instantaneous idle/busy state of the primary channel in order to detect transmission opportunities. However, the sequence of binary on/off sensing decisions can also be exploited to estimate the durations of the individual idle/busy periods observed in the primary channel until a sufficiently large set of idle/busy periods have been observed, which can then be used by the DSA/CR system to produce, based on an adequate processing of the observed period set, a broad range of primary activity statistics [7].

While many different primary activity statistics could be derived from the observed period set, the focus of this work is on the distribution of the observed idle/busy periods, which provides a complete characterisation of the statistical properties of the primary on/off activity pattern. The estimation of such distribution based on spectrum sensing observations was initially investigated in [7], where closed-form expressions were presented for the estimated distribution as a function of the original distribution and other relevant parameters such as the employed sensing period. Moreover, generic implicit closed-form expressions were also provided in [7] to quantify the error of the estimated distribution. In this context, this work extends the analytical results presented in [7] by developing an explicit closed-form expression that can be used to quantify the error of the estimated distribution under different estimation strategies. The accuracy of the obtained mathematical model is validated and corroborated with simulation results.

The rest of this work is organised as follows. First, Section II presents the considered system model and formulates the problem under study. The distribution of the observed idle/busy periods as estimated from spectrum sensing and its associated estimation error are discussed in Section III. The simulation approach considered in this work to evaluate the obtained analytical results is described in Section IV. Numerical and simulation results are presented and analysed in Section V. Finally, Section VI summarises and concludes this work.

## II. System Model and Problem Formulation

An uncertain number of primary users communicate through a radio channel targeted by the DSA/CR system. The transmissions of the primary users over the channel result in a certain activity pattern that can be modelled as a sequence of on (busy) and off (idle) periods. In general, the durations of such periods will be random and can be characterised by an

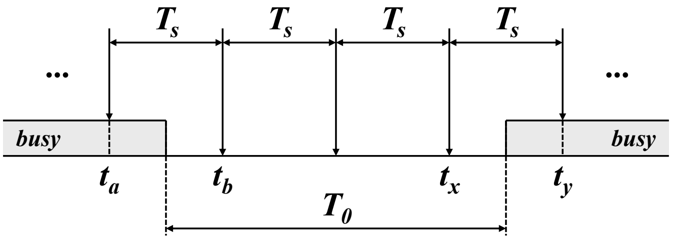


Fig. 1. Estimation of an idle period based on spectrum sensing.

appropriate distribution model. A common assumption widely used in the literature is that the idle/busy periods of the primary channel are exponentially distributed. While this assumption facilities the analytical treatment of the problem, a significant number of experimental studies have demonstrated that such assumption is unrealistic [8]–[12]. A more realistic model over a broad range of frequency bands is the Generalised Pareto (GP) distribution [13]. The Cumulative Distribution Function (CDF) of the GP distribution is given by [14, ch. 20]:

$$F_{T_i}(T) = 1 - \left[1 + \frac{\alpha_i(T - \mu_i)}{\lambda_i}\right]^{-1/\alpha_i}, \quad T \geq \mu_i \tag{1}$$

where $\mu_i > 0$, $\lambda_i > 0$ and $\alpha_i \in \mathbb{R}$ are the location, scale and shape parameters, respectively, and $T_i$ denotes the period duration ($i = 0$ for idle periods, $i = 1$ for busy periods).

The DSA/CR system is interested in estimating the distribution of the primary idle/busy periods given by (1). To this end, the idle/busy decisions of the employed spectrum sensing algorithm are used to estimate each individual idle/busy period observed in the channel as depicted in Fig. 1, where the estimation of an idle period is illustrated. The primary channel is sensed periodically by the DSA/CR system with a spectrum sensing period of $T_s$ time units (t.u.). The spectrum sensing decisions are used to determine when the primary channel changes its state (from idle to busy and vice versa). The DSA/CR system can then estimate the duration of a real idle/busy period duration, denoted as $T_i$ ($i = 0$ for idle periods, $i = 1$ for busy periods), based on the time difference between the sensing events observed around the channel state transitions ($t_a$, $t_b$, $t_x$, $t_y$ in Fig. 1). Based on the channel states observed at these sensing events, the DSA/CR system can make an estimation of the period duration, denoted as $\widehat{T}_i$, following three methods or Estimation Strategies (ESs):

- ES1: $\widehat{T}_i = t_x - t_b$ (which underestimates $T_i$).
- ES2: $\widehat{T}_i = t_y - t_a$ (which overestimates $T_i$).
- ES3: $\widehat{T}_i = \frac{(t_x - t_b) + (t_y - t_a)}{2} = t_x - t_a = t_y - t_b$ (which averages the estimations of ES1/ES2 and is expected to provide a more accurate estimation of $T_i$).

The process is repeated for each individual idle/busy period observed in the primary channel until a sufficiently large set of $N$ observed period durations is collected, which is denoted by $\widehat{\mathcal{T}}_i = \{\widehat{T}_{i,n}\}_{n=1}^{N}$. The number of periods $N$ that the DSA/CR system needs to collect to attain a certain level of accuracy is beyond the scope of this work but a detailed analysis can be found in [15]. Based on an adequate processing of the values in the set $\widehat{\mathcal{T}}_i$, the DSA/CR system can make an estimation of several primary activity statistics, including the distribution in (1). Note that the original periods $T_i$ will in general have a continuous domain while the periods $\widehat{T}_i$ estimated from sensing as shown in Fig. 1 will have a discrete domain since they are integer multiples of the sensing period ($\widehat{T}_i = kT_s$, $k \in \mathbb{N}^+$). The employed sensing period determines the accuracy to which each individual period can be estimated and therefore introduces some error in the estimated distribution. The focus of this work is on the error between the distribution estimated from the set $\widehat{\mathcal{T}}_i$ and the true distribution in (1) for each of the three considered estimation strategies.

## III. Estimated Distribution and its Accuracy

Given a set $\widehat{\mathcal{T}}_i = \{\widehat{T}_{i,n}\}_{n=1}^{N}$ of $N$ observed primary period durations, an estimation of the distribution $F_{T_i}(T)$ given in (1), which is denoted as $F_{\widehat{T}_i}(\widehat{T})$, can be made as follows:

$$F_{\widehat{T}_i}(\widehat{T}) = \frac{1}{N}\sum_{n=1}^{N} \mathbf{1}_{\widehat{\mathcal{T}}_i(\widehat{T})}\{\widehat{T}_{i,n}\} = \frac{|\widehat{\mathcal{T}}_i(\widehat{T})|}{N} \tag{2}$$

where $|\widehat{\mathcal{T}}_i(\widehat{T})|$ indicates the cardinality (number of elements) of $\widehat{\mathcal{T}}_i(\widehat{T}) = \{\widehat{T}_{i,n} : \widehat{T}_{i,n} \leq \widehat{T}, n = 1, \ldots, N\}$ (the subset of period durations lower than or equal to $\widehat{T}$), and $\mathbf{1}_A\{x\}$ is the indicator function of subset $A$, which is equal to one for the elements $x \in A$ and zero otherwise. The distribution estimated in this way is usually referred to as *empirical CDF*.

As discussed in Section II, the original distribution $F_{T_i}(T)$ in (1) will have in general a continuous domain ($T \in \mathbb{R}^+$) while the estimated distribution $F_{\widehat{T}_i}(\widehat{T})$ in (2) will always have a discrete domain ($\widehat{T} = kT_s, k \in \mathbb{N}^+$) as a result of employing a finite sensing period. The relation between the estimated distribution $F_{\widehat{T}_i}(\widehat{T})$ in (2) and the true distribution $F_{T_i}(T)$ in (1) as a function of the employed sensing period $T_s$ was investigated in [7] and was found to be given by:

$$F_{\widehat{T}_i}(\widehat{T}) = G_{\widehat{T}_i}\left(\widehat{T} + \frac{T_s}{2}\right) \tag{3}$$

where $G_{\widehat{T}_i}(\cdot)$ is given by (5) and $\Omega(\cdot)$ is given by:

$$\Omega(\tau) = \frac{[\lambda_i + \alpha_i(\tau - \mu_i)]^2}{(\alpha_i - 1)(1 - 2\alpha_i)T_s^2}[1 - F_{T_i}(\tau)] \tag{4}$$

The expressions in (3)–(5) assume that the estimation strategy ES3 is employed, however they are also valid for ES1 and ES2 by replacing $T$ with $T + T_s$ and $T - T_s$, respectively.

The error of the estimated distribution $F_{\widehat{T}_i}(\widehat{T})$ with respect to the true distribution $F_{T_i}(T)$ can be quantified in terms of the Kolmogorov-Smirnov (KS) distance, which is defined as the maximum absolute difference between the CDFs [16, eq. (14.3.17)] and in the context of this work takes the form:

$$D_i^{KS} = \sup_T \left| F_{T_i}(T) - F_{\widehat{T}_i}\left(\left\lfloor \frac{T}{T_s} \right\rfloor T_s\right)\right| \tag{8}$$

Notice that the KS distance is defined in the context of continuous distributions and therefore the expression for $F_{\widehat{T}_i}(\widehat{T})$ in

$$G_{\widehat{T}_i}(T)=\begin{cases}0, & T \le \mu_i - T_s & \text{(5a)}\\ \Omega(T+T_s)+\frac{\lambda_i^2}{(1-\alpha_i)(1-2\alpha_i)T_s^2}+\frac{T^2-(\mu_i-T_s)^2}{2T_s^2}+\left(T_s-\mu_i-\frac{\lambda_i}{1-\alpha_i}\right)\frac{T+T_s-\mu_i}{T_s^2}, & \mu_i - T_s < T \le \mu_i & \text{(5b)}\\ \Omega(T+T_s)-2\Omega(T)-\frac{\lambda_i^2}{(1-\alpha_i)(1-2\alpha_i)T_s^2}+\frac{\lambda_i}{1-\alpha_i}\frac{T-T_s-\mu_i}{T_s^2}-\frac{T^2-T_s^2-\mu_i^2}{2T_s^2}+\frac{(T-\mu_i)(T_s+\mu_i)}{T_s^2}, & \mu_i < T \le \mu_i + T_s & \text{(5c)}\\ 1+\Omega(T+T_s)-2\Omega(T)+\Omega(T-T_s), & T > \mu_i + T_s & \text{(5d)}\end{cases}$$

$$\left[1+\frac{\alpha_i(T-\mu_i)}{\lambda_i}\right]^{-1/\alpha_i+a} = 1+\sum_{m=1}^{\infty}\frac{1}{m!}\left(\frac{\alpha_i}{\lambda_i}\right)^m\left[\prod_{l=1}^{m}\left(1-l+a-\frac{1}{\alpha_i}\right)\right](T-\mu_i)^m \tag{6}$$

$$\approx 1-\left(\frac{1-a\alpha_i}{\lambda_i}\right)(T-\mu_i)+\frac{(1-a\alpha_i)(1+\alpha_i-a\alpha_i)}{2\lambda_i^2}(T-\mu_i)^2 \tag{7}$$

---

(3) has been rewritten in terms of the continuous variable $T$ (instead of the discrete variable $\widehat{T}$) before being introduced into (8) by using the relation $\widehat{T} = \lfloor T/T_s \rfloor T_s$ (where $\lfloor \cdot \rfloor$ denotes the floor function), which represents the discretisation of the continuous time domain into the discrete time domain over which the estimated distribution $F_{\widehat{T}_i}(\widehat{T})$ is defined.

The KS distance in (8) can be evaluated analytically by determining the period duration $T_i^{KS}$ for which the absolute difference of (8) is maximum and then evaluating at $T = T_i^{KS}$.

In order to find an expression for $T_i^{KS}$, let's first define:

$$T_i^* = \left\{T : \xi(T) = \sup_T \xi(T)\right\} \tag{9}$$

as the period duration in the continuous time domain for which the absolute difference between $F_{T_i}(T)$ in (1) and $F_{\widehat{T}_i}(\lfloor T/T_s \rfloor T_s)$, which is denoted as $\xi(T)$ as shown in (10), takes its maximum value.

$$\xi(T) = \left| F_{T_i}(T) - F_{\widehat{T}_i}\left(\left\lfloor \frac{T}{T_s} \right\rfloor T_s\right)\right| \tag{10}$$

The sought $T_i^*$ can be found by computing the value of $T$ for which $\partial\xi(T)/\partial T = 0$ and $\partial^2\xi(T)/\partial T^2 < 0$. The resolution of these equations for ES1 (after replacing $T$ with $T + T_s$) and for ES3 is straightforward and yields the result $T_i^* = \mu_i$ (where $\mu_i$ is the location parameter of the original distribution and represents the minimum period duration). However, the resolution of these same equations for ES2 (after replacing $T$ with $T - T_s$) is not possible as a result of the presence of non-polynomial terms arising from the algebraic form of $F_{T_i}(T)$ in (1). This problem can be overcome by replacing such non-polynomial terms with their equivalent Taylor series centred around the point $T = \mu_i$ as shown in (6) and then taking their second-order approximation as shown in (7), which yields the following tight approximation:

$$T_i^* \approx \mu_i + \frac{\vartheta_i - \sqrt{\vartheta_i^2 - 4\varphi_i/\lambda_i}}{\varphi_i}, \quad \text{for ES2} \tag{11a}$$

where

$$\vartheta_i = \frac{2}{\lambda_i T_s} + \frac{1+\alpha_i}{\lambda_i^2} \tag{11b}$$

$$\varphi_i = \frac{1}{\lambda_i T_s^2} + \frac{(1+\alpha_i)(1+2\alpha_i)}{\lambda_i^3} \tag{11c}$$

As it can be appreciated, the value of $T_i^*$ for ES2 is not constant (as it is the case of ES1 and ES3) but depends on the employed sensing period $T_s$. Moreover, it can be shown that $T_i^*$ for ES2 is comprised within the interval $[\mu_i+T_s, \mu_i+2T_s]$ provided that $T_s \le \mu_i$, which is indeed required to enable an accurate estimation of the periods and their distribution.

Based on the obtained $T_i^*$ for each estimation strategy, the desired $T_i^{KS}$ can be found by appropriately rounding $T_i^*$ to either $\lfloor T_i^*/T_s \rfloor T_s$ or $\lceil T_i^*/T_s \rceil T_s$, whichever maximises the value of $\xi(\cdot)$ in (10). Recall, as mentioned earlier in this section, that the estimated distribution $F_{\widehat{T}_i}(\widehat{T})$ in (2) has a discrete domain ($\widehat{T} = kT_s, k \in \mathbb{N}^+$) as a result of employing a finite sensing period, which also means that it is a stair-shaped function. One can intuitively realise that the comparison of such stair-shaped function with the continuous distribution of the original periods $F_{T_i}(T)$ in (1) will have the maximum absolute difference exactly at one of the steps of $F_{\widehat{T}_i}(\widehat{T})$ (i.e., at one of the discrete values of $\widehat{T}$ for which the estimated CDF is defined), which in fact is an integer multiple of the sensing period ($\widehat{T} = kT_s, k \in \mathbb{N}^+$). From the analysis performed above, such value will necessarily have to be in the immediate vicinity of the obtained $T_i^* \in \mathbb{R}^+$. Therefore, the value $T_i^{KS}$ that maximises the absolute difference $\xi(\cdot)$ in (10) will be one of the nearest integer multiples of $T_s$ around $T_i^*$, i.e., either $\lfloor T_i^*/T_s \rfloor T_s$ or $\lceil T_i^*/T_s \rceil T_s$. This leads to the problem of which of these two options is the right choice for each employed sensing period and estimation strategy. In general, there is no simple or obvious relation, however by performing an exhaustive analysis of the absolute difference $\xi(\cdot)$ in (10) in both candidate points, i.e. $\lfloor T_i^*/T_s \rfloor T_s$ and $\lceil T_i^*/T_s \rceil T_s$, and observing the point where such difference is greater, the following rounding rules for $T_i^*$ were empirically obtained:

$$T_i^{KS} \approx \begin{cases}\left\lfloor \frac{T_i^*}{T_s} \right\rfloor T_s, & \text{for ES1} & \text{(12a)}\\ \left\lfloor \frac{T_i^* + \frac{T_s}{2} - \left|\left\lfloor \frac{\mu_i}{T_s} \right\rceil T_s - \mu_i\right|}{T_s} \right\rceil T_s, & \text{for ES2} & \text{(12b)}\\ \left\lfloor \frac{T_i^* + \left|\left\lfloor \frac{\mu_i}{T_s} \right\rceil T_s - \mu_i\right|}{T_s} \right\rceil T_s, & \text{for ES3} & \text{(12c)}\end{cases}$$

where $T_i^* = \mu_i$ for ES1 and ES3, $T_i^*$ is given by (11) for ES2, and $\lfloor \cdot \rceil$ is the nearest integer (round) operator.

The introduction of the obtained $T_i^{KS}$ in (12) into (8) provides the final expression for the KS distance:

$$D_i^{KS} = \left| F_{T_i}\left(T_i^{KS}\right) - G_{\widehat{T}_i}\left(T_i^{KS} + \xi_i \frac{T_s}{2}\right)\right| \tag{13}$$

where

$$\xi_i = \begin{cases} 1, & \text{for ES1} \quad (14a) \\ -1, & \text{for ES2} \quad (14b) \\ \operatorname{sgn}\left(\left\lfloor \frac{\mu_i}{T_s} \right\rceil T_s - \mu_i\right) \times & \text{for ES3} \quad (14c) \\ \times \operatorname{sgn}\left(\left\lfloor \frac{\mu_i + \left|\left\lfloor \frac{\mu_i}{T_s} \right\rceil T_s - \mu_i\right|}{T_s} \right\rceil T_s - \mu_i\right) & \end{cases}$$

with $\operatorname{sgn}(x) = x/|x|$ being the sign function. Since the estimated distribution has discontinuities at every step (i.e., at the integer multiples of $T_s$), the term $\xi_i \in \{-1, +1\}$ is needed to indicate from which side of the discontinuity the value of the distribution is considered in (13).

## IV. Simulation Methodology

The accuracy of the mathematical models developed in Section III to quantify the error of the estimated distribution for each estimation strategy was evaluated by means of software simulations in Matlab based on the following steps:

1) Generate a sequence of $N$ alternated idle/busy periods, whose durations $T_0/T_1$ are obtained as random numbers drawn from generalised Pareto distributions.
2) From the sequence of idle/busy periods obtained in step 1, determine the sequence of idle/busy states ($\mathcal{H}_0/\mathcal{H}_1$) that would be observed in the primary channel when the channel is sensed with a sensing period $T_s$.
3) Based on the sequence $\mathcal{H}_0/\mathcal{H}_1$ obtained in step 2, compute, as depicted in Fig. 1, the period durations $\widehat{T}_0/\widehat{T}_1$ that would be observed with each of the three considered estimation strategies (ES1/ES2/ES3).
4) Calculate the empirical CDF of the period durations $\widehat{T}_0/\widehat{T}_1$ obtained in step 3 as indicated by (2).
5) Compare the estimated distribution from step 4 with the original distribution used in step 1 and quantify the estimation error in terms of the KS distance in (8).

The value of $N$ (i.e., number of simulated idle/busy periods) was selected based on the analytical results provided in [15] in order to ensure that the employed sample size $N$ was in all cases sufficiently large to remove the impact of estimating the distribution based on a limited number of observed periods.

## V. Numerical and Simulation Results

This section assesses the accuracy of the mathematical models proposed in this work by numerically evaluating the expressions developed in Section III and comparing with the corresponding results obtained by simulations as detailed in Section IV. The examples shown in this section were obtained when the generalised Pareto distribution for the true periods was configured with the following parameters: $\mu_i = 5$ t.u., $\lambda_i = 5$ t.u. and $\alpha_i = 0.1$. The conclusions obtained for this particular configuration are valid for other values as well.

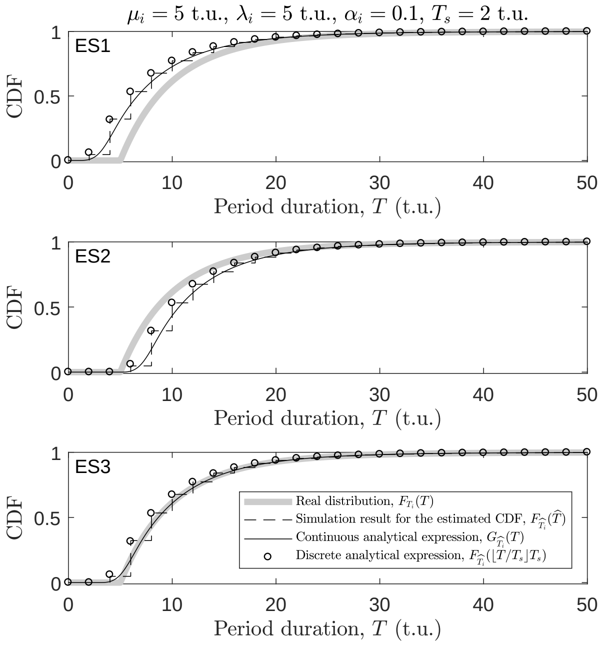


Fig. 2. Distribution of the real $T_i$ and estimated $\widehat{T}_i$ periods for the three considered estimation strategies: ES1 (top), ES2 (middle) and ES3 (bottom).

Fig. 2 compares the distribution estimated from the periods observed in the primary channel based on spectrum sensing (when the employed sensing period is $T_s = 2$ t.u.) with the distribution of the original primary idle/busy periods. As it can be appreciated, while the original distribution is continuous, the estimated distribution is discrete regardless of the employed estimation strategiy (hence the stair shape). As discussed in Section III, this stair shape is an inherent consequence of estimating the individual idle/busy periods based on spectrum sensing and, as a result, it can also be observed that the step width of the estimated distribution is equal to the employed sensing period ($T_s = 2$ t.u. in the example of Fig. 2); since all the estimated periods are integer multiples of the sensing period, their (discrete) distribution is defined only for values that are integer multiples of the employed sensing period as well.

The fact that the estimated distribution has a discrete domain will necessarily introduce an estimation error with respect to the original distribution, which is continuous. This estimation error could be reduced by reducing the employed sensing period, which would also reduce the step width of the estimated distribution and would therefore make it look more similar to the original distribution. However, the estimation error is affected not only by the employed sensing period but also by the employed estimation strategy. The estimated distributions observed in Fig. 2 are in line with the observations made in Section II when the three considered estimation strategies were

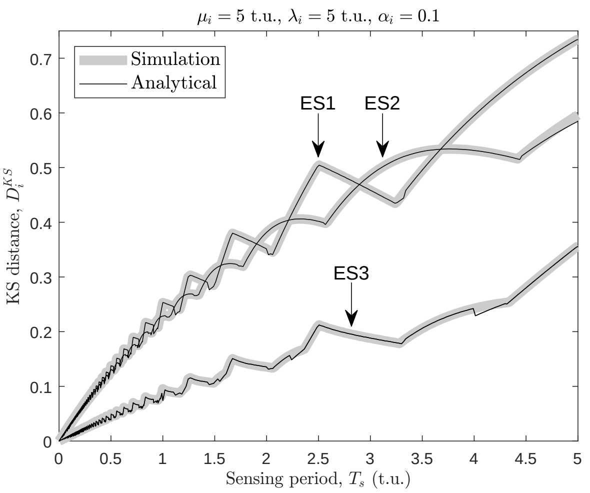


Fig. 3. Accuracy of the three considered estimation strategies.

introduced. When ES1 is employed, the estimated periods will be shorter than the original periods and as a result the distribution estimated with ES1 is shifted to the left of the original distribution in Fig. 2. Similarly, ES2 results in estimated periods that are longer than the original periods and consequently the distribution estimated in this case is shifted to the right of the original distribution in Fig. 2. Moreover, the periods estimated with ES3 can be thought of as the average of the periods estimated by ES1 and ES2, which leads to an estimated distribution that lies in between. Moreover, the points of the distribution estimated with ES3 are closer to those of the original distribution and as a result it can be stated that ES3 provides the most accurate estimation.

The accuracy of the distribution obtained with each estimation strategy can be evaluated numerically with the mathematical models developed in Section III. Fig. 3 compares the accuracy results obtained from the proposed mathematical models with those obtained from simulations. As it can be appreciated, the results shown in Fig. 3 provide quantitative evidence of the claims made above about the possibility to reduce the estimation error by reducing the employed sensing period and/or using ES3 instead of ES1 or ES2 (as a matter of fact, the estimation error of ES3 is roughly about one half the error obtained with ES1 and ES2). More importantly, the results shown in Fig. 3 demonstrate that there exists a nearly perfect agreement between analytical and simulation results for the three considered estimation strategies over the whole range of considered sensing periods ($T_s \leq \mu_i$), which demonstrates the validity and remarkable accuracy of the mathematical models developed in this work.

## VI. Conclusions

DSA/CR systems can benefit from the knowledge of primary activity statistics such as the distribution of idle/busy periods. Such statistics can be estimated based on the outcomes of the spectrum sensing process, but will be affected by a certain estimation error that depends on the employed sensing period as well as the selected estimation strategy. In this context, this work has proposed closed-form mathematical models that can be used to quantify the error of the estimated distribution as a function of the parameters of the original distribution and the employed sensing period. The validity of the proposed models has been corroborated with simulation results, which demonstrate that the proposed mathematical models provide an excellent level of accuracy. These models constitute a valuable tool that can find useful applications in performance evaluations and system designs (e.g., to calculate the maximum sensing period required to guarantee a minimum level of accuracy for a particular statistical distribution of the primary idle/busy periods).


## Acknowledgements

This work was supported by British Council under UKIERI DST Thematic Partnerships 2016-17 (ref. DST-198/2017).


## References


[1] M. M. Buddhikot, "Understanding dynamic spectrum access: Taxonomy, models and challenges," in *Proc. 2nd IEEE Int'l. Symp. Dyn. Spect. Access Networks (DySPAN 2007)*, Apr. 2007, pp. 649–663.

[2] Y.-C. Liang, K.-C. Chen, G. Y. Li, and P. Mähönen, "Cognitive radio networking and communications: An overview," *IEEE Trans. Vehic. Tech.*, vol. 60, no. 7, pp. 3386–3407, Sep. 2011.

[3] M. López-Benítez, "Cognitive radio," in *Heterogeneous cellular networks: Theory, simulation and deployment*. Cambridge University Press, 2013, ch. 13.

[4] Y. Chen and H.-S. Oh, "Spectrum measurement modelling and prediction based on wavelets," *IET Communications*, vol. 10, no. 16, pp. 2192–2198, Oct. 2016.

[5] J. Vartiainen, M. Höyhtyä, J. Lehtomäki, and T. Bräysy, "Priority channel selection based on detection history database," in *Proc. Fifth Int'l. Conf. Cognitive Radio Oriented Wireless Networks & Comms. (CROWNCOM 2010)*, Jun. 2010, pp. 1–5.

[6] K. W. Sung, S.-L. Kim, and J. Zander, "Temporal spectrum sharing based on primary user activity prediction," *IEEE Trans. Wireless Comms.*, vol. 9, no. 12, pp. 3848–3855, Dec. 2010.

[7] M. López-Benítez, A. Al-Tahmeesschi, D. K. Patel, J. Lehtomäki, and K. Umebayashi, "Estimation of primary channel activity statistics in cognitive radio based on periodic spectrum sensing observations," *IEEE Trans. Wireless Comms.*, vol. 18, no. 2, pp. 983–996, Feb. 2019.

[8] S. Geirhofer, L. Tong, and B. M. Sadler, "A measurement-based model for dynamic spectrum access in WLAN channels," in *Proc. IEEE Military Comms. Conf. (MILCOM 2006)*, Oct. 2006, pp. 1–7.

[9] ——, "Dynamic spectrum access in WLAN channels: Empirical model and its stochastic analysis," in *Proc. First Int'l. Works. Tech. and Policy for Accessing Spect. (TAPAS 2006)*, Aug. 2006, pp. 1–10.

[10] ——, "Dynamic spectrum access in the time domain: Modeling and exploiting white space," *IEEE Comms. Mag.*, vol. 45, no. 5, pp. 66–72, May 2007.

[11] L. Stabellini, "Quantifying and modeling spectrum opportunities in a real wireless environment," in *Proc. IEEE Wireless Comms. and Networking Conf. (WCNC 2010)*, Apr. 2010, pp. 1–6.

[12] M. Wellens, J. Riihijärvi, and P. Mähönen, "Empirical time and frequency domain models of spectrum use," *Physical Comm.*, vol. 2, no. 1-2, pp. 10–32, Mar. 2009.

[13] M. López-Benítez and F. Casadevall, "Time-dimension models of spectrum usage for the analysis, design and simulation of cognitive radio networks," *IEEE Trans. Vehic. Tech.*, vol. 62, no. 5, pp. 2091–2104, Jun. 2013.

[14] N. L. Johnson, S. Kotz, and N. Balakrishnan, *Continuous univariate distributions*, 2nd ed. Wiley, Nov. 1994, vol. 1.

[15] A. Al-Tahmeesschi, M. López-Benítez, D. K. Patel, J. Lehtomäki, and K. Umebayashi, "On the sample size for the estimation of primary activity statistics based on spectrum sensing," *IEEE Trans. Cognitive Comms. and Networking*, vol. 5, no. 1, pp. 59–72, Mar. 2019.

[16] W. H. Press, S. A. Teukolsky, W. T. Vetterling, and B. P. Flannery, *Numerical recipes: The art of scientific computing*, 3rd ed. Cambridge University Press, 2007.